Different Effects of Long- and Short-Chain Ceramides on the Gel-Fluid and Lamellar-Hexagonal Transitions of Phospholipids: A Calorimetric, NMR, and X-Ray Diffraction Study

Jesús Sot,* Francisco J. Aranda,† M.-Isabel Collado,‡ Félix M. Goñi,* and Alicia Alonso*
*Unidad de Biofísica (Centro Mixto CSIC-UPV/EHU) and Departamento de Bioquímica, Universidad del País Vasco, 48080 Bilbao, Spain; †Departamento de Bioquímica y Biología Molecular A, Facultad de Veterinaria, Universidad de Murcia, Murcia, Spain; and ‡Servicio General de Resonancia Magnética Nuclear, Universidad del País Vasco, Bilbao, Spain

ABSTRACT The effects on dielaidoylphosphatidylethanolamine (DEPE) bilayers of ceramides containing different N-acyl chains have been studied by differential scanning calorimetry small angle x-ray diffraction and ^{31}P-NMR spectroscopy. *N*-palmitoyl (Cer16), *N*-hexanoyl (Cer6), and *N*-acetyl (Cer2) sphingosines have been used. Both the gel-fluid and the lamellar-inverted hexagonal transitions of DEPE have been examined in the presence of the various ceramides in the 0-25 mol % concentration range. Pure hydrated ceramides exhibit cooperative endothermic order-disorder transitions at 93°C (Cer16), 60°C (Cer6), and 54°C (Cer2). In DEPE bilayers, Cer16 does not mix with the phospholipid in the gel phase, giving rise to high-melting ceramide-rich domains. Cer16 favors the lamellar-hexagonal transition of DEPE, decreasing the transition temperature. Cer2, on the other hand, is soluble in the gel phase of DEPE, decreasing the gel-fluid and increasing the lamellar-hexagonal transition temperatures, thus effectively stabilizing the lamellar fluid phase. In addition, Cer2 was peculiar in that no equilibrium could be reached for the Cer2-DEPE mixture above 60°C, the lamellar-hexagonal transition shifting with time to temperatures beyond the instrumental range. The properties of Cer6 are intermediate between those of the other two, this ceramide decreasing both the gel-fluid and lamellar-hexagonal transition temperatures. Temperature-composition diagrams have been constructed for the mixtures of DEPE with each of the three ceramides. The different behavior of the long- and short-chain ceramides can be rationalized in terms of their different molecular geometries, Cer16 favoring negative curvature in the monolayers, thus inverted phases, and the opposite being true of the micelle-forming Cer2. These differences may be at the origin of the different physiological effects that are sometimes observed for the long- and short-chain ceramides.

INTRODUCTION

Ceramides (*N*-acylsphingosines) have been known for decades as intermediates in sphingolipid metabolism and as minor membrane components (Stoffel, 1971; Wiegandt, 1970), and their structure and physical properties have been described (Pascher, 1976). However, the relatively recent realization that ceramides are powerful metabolic signals involved in many cell physiological and pathophysiological events (see Cremesti et al., 2002; Van Blitterswijk et al., 2003, for reviews) has attracted renewed attention to these molecules. From the point of view of their physical properties, they have been studied both alone and in combination with phospholipids (see Kolesnick et al., 2000 for a review).

The interaction of ceramides with phospholipids is important because it is believed to constitute the basis of several phenomena of potential physiological significance, namely the ceramide-dependent increase in membrane permeability (Montes et al., 2002; Ruiz-Argüello et al., 1996; Siskind and Colombini, 2000; Siskind et al., 2002), formation of transient nonlamellar structures in membranes (Ruiz-Argüello et al., 1996, 1998; Veiga et al., 1999), transbilayer lipid motion (Contreras et al., 2003, 2005), and lateral segregation of ceramide-enriched domains (Carrer and Maggio, 1999; Holopainen et al., 1997, 1998; Hsueh et al., 2002; Huang et al., 1996, 1998; Veiga et al., 1999). Ceramide-phospholipid interaction, and, in general, lipid-lipid interaction, is often studied by examining the effects of one lipid (e.g., ceramide) on the thermotropic phase properties of the other (e.g., a phospholipid). This procedure has been used in the recent past with a variety of techniques and lipids. Massey (2001) used the fluorescence properties of diphenylhexatriene, prodan, and laurdan to study the gel-fluid phase transitions of dipalmitoylphosphatidylcholine (DPPC) and of various natural sphingomyelins and their modification by several natural and synthetic long-chain ceramides. Veiga et al. (1999) applied infrared (IR) spectroscopy to the study of deuterated DPPC bilayers and the effect of brain ceramide on their gel-fluid transition. Other authors have used differential scanning calorimetry (DSC) in studies of natural ceramides and DPPC (Carrer and Maggio, 1999; Carrer et al., 2003) or dielaidoylphosphatidylethanolamine (DEPE; Veiga et al., 1999). The lamellar-hexagonal thermotropic transition and ceramide effects thereupon have been explored by DSC, using egg ceramide and DEPE (Veiga et al., 1999), and by 31P-NMR, using a mixture of natural lipids and egg ceramide (Ruiz-Argüello et al., 1996; Veiga et al., 1999).

This study reports on the effects of three chemically defined ceramides, namely *N*-hexadecanoylsphingosine (Cer16),

Submitted December 14, 2004, and accepted for publication January 25, 2005.

Address reprint requests to Alicia Alonso, Fax: 34-94-601-3360; E-mail: gbpaliza@lg.ehu.es.

0006-3495/05/05/3368/13 $2.00

doi: 10.1529/biophysj.104.057851

N-hexanoylsphingosine (Cer6), and *N*-acetylsphingosine (Cer2), on the gel-fluid and lamellar-inverted hexagonal thermotropic phase transitions of DEPE, a phospholipid whose respective transitions, when in the pure state, occur respectively at $T_m \approx 37.5°C$ and $T_h \approx 65°C$ (Veiga et al., 1999). The range of ceramide concentrations under study has been of 0–24 mol % (mole fraction 0.00–0.24 with respect to total lipid) in most cases, considering that higher ceramide proportions are not likely to occur under physiological conditions. The transitions have been studied by high-sensitivity DSC, a probe-free procedure that can be applied to physiological low concentrations of lipids in water dispersions, whereas lipid phases have been identified using small angle x-ray diffraction and ^{31}P-NMR spectroscopy, both well-tested, nonprobe-requiring techniques. Short-chain (Cer2 and Cer6) ceramides have not been examined in the past in the context of phospholipid phase transitions, apart from a preliminary study of *N*-octanoylsphingosine by Carrer et al. (2003). Some physical properties of short-chain ceramides differ widely from those of their long-chain counterparts; e.g., short-chain ceramides can be easily dispersed in water, whereas long-chain ones can hardly be hydrated, let alone be homogeneously dispersed (Sot et al., 2005). The physiological effects of short-chain ceramides are often, but not always, similar to those of the long-chain ones (Di Paola et al., 2000; Guidoni et al., 1999; Kolesnick et al., 2000). The DSC studies shown below reveal profound differences in the mode of interaction of the various ceramides with a phospholipid, depending on the N-acyl chain length.

MATERIALS AND METHODS

Materials

1,2-Dielaidoyl-*sn*-glycero-3-phosphoethanolamine (DEPE), *N*-palmitoyl-D-erythro-sphingosine (Cer16), *N*-hexanoyl-D-erythro-sphingosine (Cer6), and *N*-acetyl-D-erythro-sphingosine (Cer2) were supplied by Avanti Polar Lipids (Alabaster, AL). All of these lipids were >99% pure according to the suppliers and were used without further purification.

Liposome preparation

For liposome preparation, DEPE and ceramides were dissolved in chloroform:methanol (2:1, v/v), and the mixture was evaporated to dryness under a stream of nitrogen. Traces of solvent were removed by evacuating the samples under high vacuum for at least 2 h. The samples were hydrated at 45°C in 20 mM PIPES, 150 mM NaCl, 1 mM EDTA, pH 7.4, helping dispersion by stirring with a glass rod. To ensure homogeneous dispersions, the hydrated samples were extruded between two syringes through a narrow tubing (0.5 mm internal diameter, 10 cm long) 100 times at 45°C. In these samples, the amount of phospholipid was kept constant, whereas the amount of ceramides and, correspondingly, that of total lipid varied.

DSC measurements

Both lipid suspensions and buffer were degassed before being loaded into the sample or reference cell of an MC-2 high-sensitivity scanning calorimeter (MicroCal, Northampton, MA). The final concentration of phospholipid was 0.4 mM for samples in which gel-to-fluid transitions were measured and 7 mM for those in which fluid-to-inverted hexagonal transitions were studied. Three heating scans, at 45°C/h, were recorded for each sample. Lipid phosphorous assays were carried out on all DEPE-containing samples after the DSC scans to obtain accurate ΔH values (in kcal/mole of phospholipid). Thermogram transition temperatures, enthalpies, and widths at half-height were determined using the software ORIGIN (Microcal) provided with the calorimeter.

For curve fitting, the software GRAMS_32 Spectra Notebase (Galactic Industries, Waltham, MA) was used (www.thermo.com/eThermo/CMA/PDFs/Product/productPDF_24179.pdf). Thermograms were fitted to the smallest number of Gaussian curves compatible with a statistically convergent solution with an R^2 correlation coefficient ≥ 0.99. The minimum number of components was two for the gel-fluid transition of the DPPE-Cer16 mixtures and for the L_α-H_{II} transition of the DEPE-Cer6 mixtures, three for the gel-fluid transition of the DEPE-Cer2 mixtures, and five for the gel-fluid transition of the DEPE-Cer6 mixtures. For instance, in the case of DEPE-Cer6 mixtures, the 24% Cer6 thermograms could be fitted to five components with $R^2 = 0.999$, but fitting to four components converged only ''at a minimum''; the 5% Cer6 thermograms could be fitted to five curves with $R^2 = 0.999$, but a four-curve solution did not converge. In systems containing DEPE-Cer2, fitting the 24% Cer2 thermogram to three curves converged with $R^2 = 0.996$, but converged only ''at a minimum'' with two components. The 5% Cer2 thermogram fitted to three curves converged with $R^2 = 0.995$, and again converged ''at a minimum'' when a two-curve fitting was attempted.

X-ray diffraction measurements

Small angle x-ray diffraction (SAX) measurements were carried out using a Kratky compact camera (MBraum-Graz-Optical Systems, Graz, Austria) and a linear position sensitive detector (PSD; MBraum, Garching, Germany) monitoring the *s*-range ($s = 2 \sin\theta/\lambda$, 2θ = scattering angle, $\lambda = 1{,}54$ Å) between 0.0075 and 0,07 Å^{-1}. Nickel-filtered Cu K_α x-rays were generated by a Philips (Eindhoven, The Netherlands) PW3830 x-ray generator operating at 50 kV and 30mA. The position calibration of the detector was performed by using Ag-stearate (d-spacing at 48.8Å) as reference material. Samples for x-ray diffraction were prepared by mixing 15 mg of DEPE and the appropriate amount of ceramides in chloroform/methanol (2:1). Liposomes were prepared as described above. After centrifugation at 13,000 rpm, the pellets were measured in a steel holder with cellophane windows, which provides good thermal contact to the Peltier heating unit. X-ray diffraction profiles were obtained for 5 min exposure times after 10 min of temperature equilibration.

NMR measurements

^{31}P-NMR spectra were recorded in a Bruker (Rheinstetten, Germany) AV500 spectrometer operating at 500 MHz for protons (202.4 MHz for ^{31}P). The final phospholipid concentration was 100 mM. Spectral parameters were 45° pulses (11.5 μs), pulse interval of 1s, sweep width of 30 kHz, and full proton decoupling. Two thousand free induction decays were routinely accumulated from each sample; the spectra were plotted with a line broadening of 40 Hz. Samples were equilibrated for at least 10 min at each temperature before data acquisition.

RESULTS AND DISCUSSION

Ceramides in buffer

Cer16, Cer6, and Cer2 displayed narrow, reversible endothermic transitions (thermograms not shown) probably between an ordered and a disordered state (Moore and Rerek,

1997). Cer16 was highly insoluble in water; its thermal properties could only be studied in heterogeneous dispersions obtained by forcing the lipid-buffer mixture through a narrow tubing multiple times. The midpoint transition temperature of Cer16 was $T_m = 93.2°C$, and the transition enthalpy was $\Delta H = 4.5$ Kcal/mol. T_m was in agreement with previous DSC data (Han et al., 1995; Shah et al., 1995). Moore and Rerek (1997) observed similar order-disorder transitions by IR spectroscopy in ceramides of natural origin. Shah et al. (1995) reported a higher ΔH value (13.5 Kcal/mol) for the Cer16 endotherm, and an exotherm at ~64°C that was not detected in our case. We attribute these noncoincident observations to differences in sample preparation. In particular the much higher sample volume in the instrument used in this study versus the one used by Shah et al. allows the use of extrusion in the sample preparation procedure, which in turn ensures a better degree of hydration and a more homogeneous dispersion, within the limited dispersibility of Cer16 samples.

Cer6 and Cer2 could be easily hydrated and dispersed in buffer, the thermodynamic parameters of the corresponding thermotropic transitions were the following: for Cer6, $T_m = 59.6°C$, $\Delta H = 3.9$ Kcal/mol; for Cer2, $T_m = 54.2°C$, $\Delta H = 6.3$ Kcal/mol. Note the large difference in T_m between the hydrophobic Cer16 and the two more hydrophilic, short-chain ceramides Cer6 and Cer2. However, ΔH of Cer6 is more similar to that of Cer16 than to the corresponding value of Cer2. As discussed below, Cer6 often has intermediate properties between the long- and short-chain ceramides.

DEPE-Cer16 mixtures

Representative thermograms of the gel-fluid transition of pure DEPE and DEPE-Cer16 mixtures are shown in Fig. 1. They were very similar to those published by Veiga et al. (1999) for DEPE-egg ceramide mixtures. (Note that Cer16 is the main molecular species in egg ceramide.) The main effect of Cer16 was to broaden the gel-fluid transition of DEPE without major changes in the onset temperature. The narrow endotherm seen at the high-T side of the thermograms for 20% and 24% Cer16 corresponded to the lamellar-hexagonal transition of DEPE, as will be detailed below. This merging of the gel-fluid and lamellar-hexagonal transitions had not been noted by Veiga et al. (1999).

Cer16 at and above 5 mol % gave rise to clearly asymmetric endotherms that could be resolved into two main components (Fig. 1). Component 3 in Fig. 1 corresponded to the L_α-H_{II} transition, see below. Component 2 increases with ceramide concentration at the expense of component 1. Veiga et al. (1999), on the basis of IR spectroscopic observations of mixtures containing egg ceramide and fully deuterated DPPC, attributed components 1 and 2, respectively, to ceramide-poor and ceramide-enriched domains. Qualitatively similar conclusions were reached by Carrer and Maggio (1999) in their DSC studies of DPPC-egg ceramide mixtures.

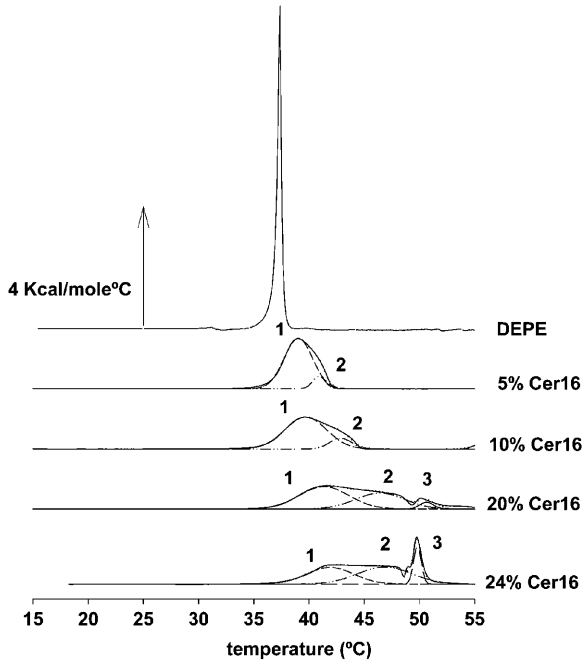

FIGURE 1 DSC thermograms corresponding to the gel-fluid transition of pure DEPE and DEPE-Cer16 mixtures in aqueous medium (third heating scans). DEPE concentration was constant (0.4 mM) in all samples. Thermograms showing complex band shapes were decomposed with the GRAMS software.

The thermodynamic parameters of the gel-fluid transition of DEPE-Cer16 mixtures are summarized in Fig. 2. In the ceramide concentration range under study, the overall ΔH of the transition remained virtually constant, although the respective contributions of components 1 and 2 varied significantly (Fig. 2 *A*), confirming the conclusions reached from visual inspection of Fig. 1. T_m of both component endotherms increased with Cer16 concentration (Fig. 2 *B*), as expected from the high melting point of pure Cer16. Transition widths also increased with Cer16 concentration (Fig. 2 *C*) due to the loss of cooperativity that is inherent to lipid domain formation. Massey (2001), using fluorescence probe techniques, had also observed increased T_m and $\Delta T_{1/2}$ in the gel-fluid transition of DPPC in the presence of bovine brain ceramide.

Perhaps the main conclusion to be derived from the thermograms and data in Figs. 1 and 2 is the low miscibility of Cer16 in DEPE bilayers. The fact that the onset transition temperature remains virtually unchanged with ceramide (Fig. 1) reveals that Cer16 does not mix with DEPE in the gel phase, and the asymmetric thermogram indicates the presence of ceramide-rich and -poor domains in the bilayer. This property of long-chain ceramides was discussed in the review by Kolesnick et al. (2000). Ceramide-rich domains were first observed by Huang et al. (1996), using ^{2}H-NMR, and later by Holopainen et al. (1997) by means of fluorescence probes, and Carrer and Maggio (1999) by DSC, among other authors. A more recent study by Hsueh et al.

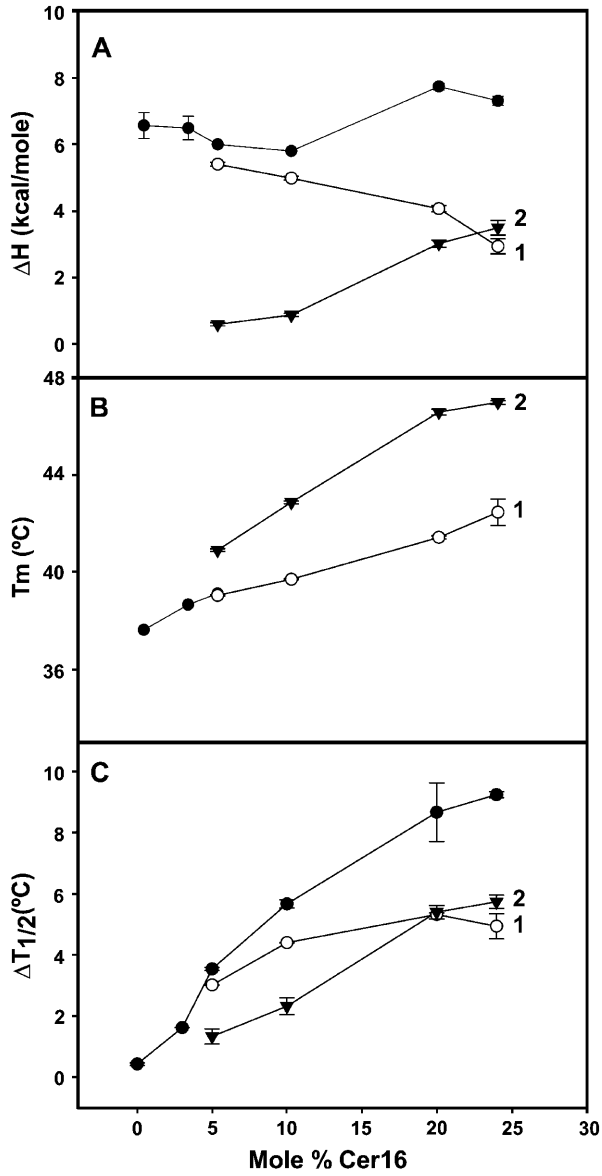

FIGURE 2 Thermodynamic parameters of the L_β-L_α transition of pure DEPE and DEPE-Cer16 mixtures in aqueous medium. (*A*) Transition enthalpy change, ΔH. (*B*) Midpoint transition temperature, T_m. (*C*) Transition width at midheight, $\Delta T_{1/2}$. (●) Data from the overall endotherm. (○) Component 1. (▼) Component 2. Average values ± SD ($n = 3$).

(2002) uses ^{2}H-NMR to examine the L_β-L_α transition of POPC-Cer16 mixtures. Their and our own data are in good agreement in that in both systems phospholipid-ceramide bilayers display gel-gel immiscibility at low temperatures. Cer16 increases the transition temperature of the system, and both components mix well in the fluid phase, at least below 20 mol % ceramide.

As mentioned in the Introduction, DEPE exhibits, in addition to the L_β-L_α transition, a lamellar-to-inverted hexagonal (L_α-H_{II}) transition within a convenient range of temperatures. The effect of Cer16 on the L_α-H_{II} transition of DEPE can be seen in the representative thermograms presented in Fig. 3. The endotherm corresponding to pure DEPE presented a high-temperature shoulder, already described by previous authors, whose origin remains obscure. This shoulder became more prominent in the presence of Cer16; however, the main ceramide effect was to lower the T_h, thus facilitating the lamellar-hexagonal transition. At ~15% Cer16, the onset of the L_α-H_{II} transition became close to the endpoint of the L_β-L_α transition. Both transitions partially overlapped at and above 20% Cer16 (see Fig. 3, *bottom thermogram*), indicating that at these ceramide concentrations, no pure L_α phase exists, and that a direct gel-to-hexagonal transition may occur.

Because of this partial overlapping of phase transitions, thermodynamic parameters of the L_α-H_{II} transition could be reliably measured only up to 10% Cer16. The data in Fig. 4 provided quantitative information on the decrease of the T_h transition temperature and increase in transition width, in the absence of significant changes in ΔH. Again these results were very similar to those published by Veiga et al. (1999) for the DEPE-egg ceramide system.

Information on the structural organization of the DEPE/Cer16 systems was obtained by the use of SAX. This technique not only defines the macroscopic structure itself, but also provides the interlamellar repeat distance in the lamellar phase. The largest first-order reflection component corresponds to the interlamellar repeat distance, which is comprised of the bilayer thickness and the thickness of the water layer between bilayers. Fig. 5 shows the diffraction patterns corresponding to pure DEPE and DEPE containing Cer16 at different temperatures. Lipids organized in multilamellar structures are expected to give rise to reflections with distances that relate as 1: 1/2: 1/3... (Luzzati, 1968).

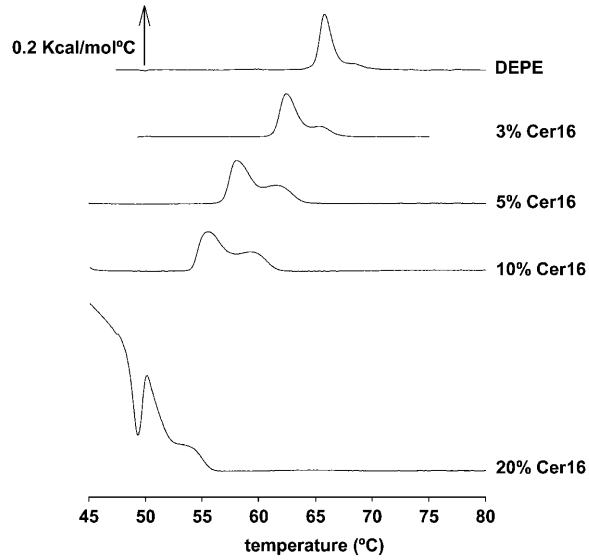

FIGURE 3 DSC thermograms corresponding to the lamellar-to-inverted hexagonal transition of pure DEPE and DEPE-Cer16 mixtures in aqueous medium (third heating scans). DEPE concentration was constant (7 mM) in all samples.

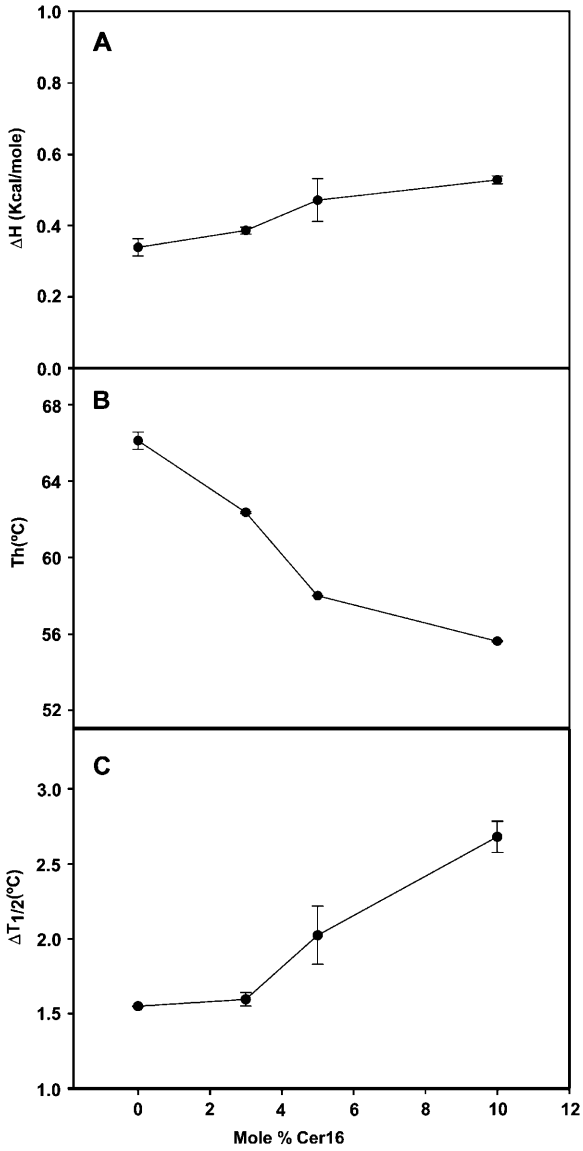

FIGURE 4 Thermodynamic parameters of the L_α-H_{II} transition of pure DEPE and DEPE-Cer16 mixtures in aqueous medium. (*A*) Transition enthalpy change, ΔH. (*B*) Midpoint hexagonal transition temperature, T_h. (*C*) Transition width at midheight, $\Delta T_{1/2}$. Average values ± SD ($n = 3$).

Pure DEPE (Fig. 5 *A*) in the lamellar gel state (30°C) showed the characteristic first-order reflection with an interlamellar repeat distance of ~64.1 Å. It has been previously observed (Killian and de Kruijff, 1985; Ortiz and Aranda, 1999) that in DEPE systems in the lamellar state, some higher-order reflections are not found. Pure DEPE in the fluid lamellar state (50°C) showed a first-order reflection with a repeat distance of ~52.6 Å. The transition to a liquid-crystalline phase was accompanied by a decrease of ~10 Å in first-order repeat distance, due to the decrease in the effective acyl chain length. Lipids organized in hexagonal H_{II} structures give rise to reflections at distances which relate as 1: $1/\sqrt{3}$: $1/\sqrt{4}$: $1/\sqrt{7}$... (Luzzati, 1968). In our case, pure DEPE in the hexagonal H_{II} phase (67°C) clearly showed the reflections characteristic of this phase (first-order reflection at ~63 Å). The repeat distances in the lamellar and hexagonal H_{II} phases were not significantly affected by the presence of the different ceramides. The presence of 10 mol % Cer16 (Fig. 5 *B*) produced the appearance of reflections characteristic of lipid organized in hexagonal H_{II} structures at 64°C, the temperature at which pure DEPE was organized in the lamellar liquid-crystalline state. When the concentration of Cer16 was increased to 24 mol % (Fig. 5 *C*), the hexagonal H_{II} diffraction pattern appeared even at lower temperatures (55°C). Interestingly, the diffraction pattern of samples containing 24 mol % Cer16 (Fig. 5) clearly showed a reflection at ~40 Å which is not present in the case of pure DEPE. A closer look at the diffraction region between 60 Å and 10 Å is presented in Fig. 6. Fig. 6 *A* shows the third- and fourth-order reflections characteristic of the DEPE organized in the lamellar gel phase and in addition two new reflections located at ~40.8 Å and ~13.6 Å which can be assigned to the first- and third-order reflections of a different lamellar phase. These reflections were more evident as more Cer16 was present in the system. Fig. 6 *B* shows that when the lipid was organized in the hexagonal H_{II} phase (second-, third-, fourth-, fifth-, and sixth-order reflections are seen), the reflections corresponding to this new lamellar phase are still present (reflections located at 43.8 Å and 14.6 Å).

The phase structure of pure DEPE and DEPE-Cer16 mixtures was also explored using ^{31}P-NMR spectroscopy. A summary of results can be seen in Fig. 7. Spectra corresponding to pure DEPE are shown in Fig. 7 *A*. At 24°C, well below the L_β-L_α transition temperature, the very wide (≈75 ppm), asymmetric lineshape with a low-field shoulder is characteristic of the L_β or gel phase. At 41°C, the spectral line is much narrower (≈50 ppm), indicating that a L_β-L_α transition has taken place. The L_α phase predominates at least up to 56°C, whereas at 61°C the characteristic lineshape of the H_{II} phase is observed. Note that, according to DSC data (Fig. 4 *B*), the L_α-H_{II} transition of pure DEPE occurs only at ~65°C. Differences in the absolute temperatures at which the transitions are detected by DSC and by ^{31}P-NMR have been observed previously for DEPE (Veiga et al., 1999) and attributed either to the different heating rates and lipid concentrations used in each technique, or to sample inhomogeneities, or to reasons intrinsic to the resonance technique (Epand and Lemay, 1993). The presence of 24% Cer16 changed markedly the phase behavior of the mixture (Fig. 7 *B*), mainly because the H_{II} phase was present already at 50°C, and clearly predominant at and above 55°C, in agreement with the x-ray diffraction and DSC data.

The data in Figs. 1–77 could be used to construct the phase diagram or, more precisely, the temperature-composition diagram in Fig. 8. To our knowledge, no such detailed phase diagram was available from previous studies. In this diagram, phase boundaries were assumed to be given by the onset and completion temperatures of the phase transitions

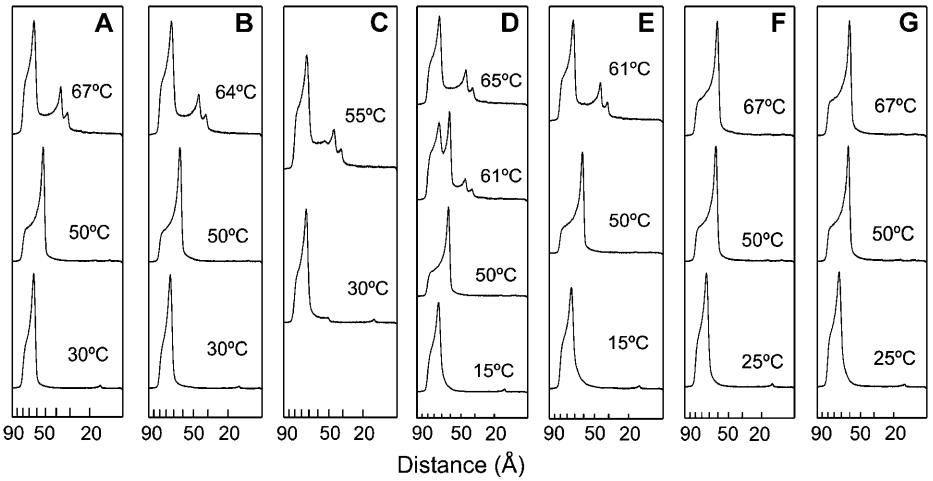

FIGURE 5 SAX profiles obtained for pure DEPE (*A*), DEPE containing 10 mol % of Cer16 (*B*), DEPE containing 24 mol % of Cer16 (*C*), DEPE containing 10 mol % of Cer6 (*D*), DEPE containing 24 mol % of Cer6 (*E*), DEPE containing 10 mol % of Cer2 (*F*), and DEPE containing 24 mol % of Cer2 (*G*), at different temperatures.

revealed by the thermograms. The onset temperature of the gel-fluid transition of DEPE (≈37°C) was virtually unchanged in the presence of ceramide, indicating that Cer16 did not mix with DEPE in the gel phase. Thus in this region of the diagram, two gel phases coexisted, a ceramide-rich one, C, and an L_β phase consisting mainly of DEPE. Gel phase immiscibility had been proposed for a similar system (DPPC-egg ceramide) by Carrer and Maggio (1999). Also in agreement with these authors, the completion temperatures of the gel-fluid phase transitions in Fig. 8 increased with Cer16 concentration, indicating that ceramide was solubilized in the fluid phase of DEPE at all concentrations up to 20 mol % Cer16. Our data are also in agreement with those published by Hsueh et al. (2002) for POPC-Cer16 mixtures.

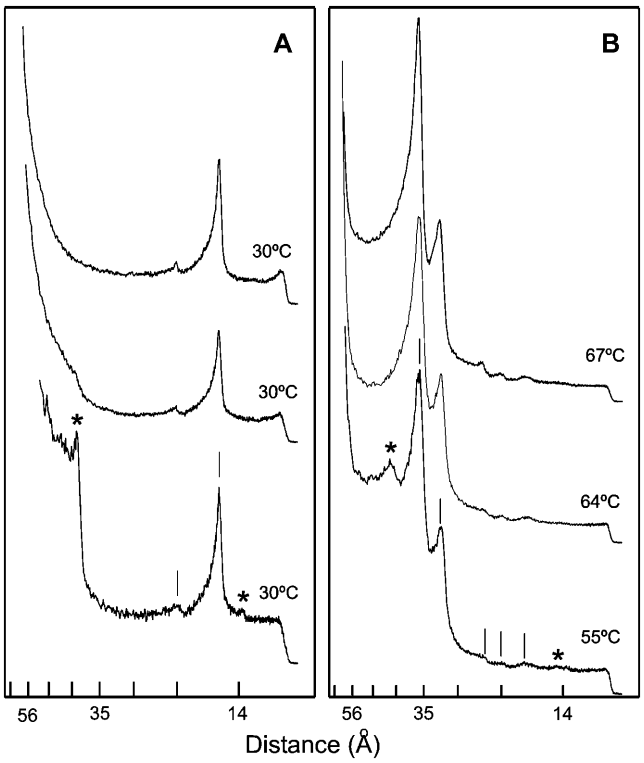

FIGURE 6 Amplification of the 60–10 Å region of the diffraction profiles obtained for pure DEPE (*top*), DEPE containing 10 mol % Cer16 (*center*), and DEPE containing 24 mol % Cer16 (*bottom*) at different temperatures. (*A*) The bars indicate the peaks corresponding to the third- and fourth-order reflections of the DEPE lamellar gel phase, and the asterisks indicate the first- and third-order reflection of a different lamellar phase obtained in the presence of Cer16. (*B*) The bars indicate the peaks corresponding to the second-, third-, fourth-, fifth-, and sixth-order reflections of the DEPE hexagonal H_{II} phase and the asterisks indicate the first- and third-order reflections of the lamellar phase obtained in the presence of Cer16.

At higher temperatures (≈65°C), pure DEPE underwent a further phase transition, from liquid-crystalline (L_α) to inverted hexagonal (H_{II}). Cer16 was solubilized in fluid DEPE and decreased the L_α-H_{II} transition temperature in a dose-dependent way. At ≈20 mol % Cer16, the onset of the L_α-H_{II} transition overlapped with the completion of the gel-fluid transition at ≈48°C so that, as mentioned above, in this region of the phase diagram (> 20 mol % Cer16) no pure L_α phase existed, and a direct gel-to-inverted hexagonal transition was possible. This kind of direct transition had also been observed in phosphatidylethanolamine-diacylglycerol mixtures (Basañez et al., 1996; Castresana et al., 1992). As discussed in our previous publications (Kolesnick et al., 2000; Veiga et al., 1999) long-chain ceramides have the propensity to stabilize inverted phases because of their geometry (Israelachvili et al., 1980), or, in the model of Helfrich (1973), long-chain ceramides tend to increase the ''negative curvature'' of lipid monolayers, thus facilitating inverted phase formation. See also Siegel and Epand (1997) on the mechanism of L_α-H_{II} transitions in phosphatidylethanolamines.

DEPE-Cer6 mixtures

The effect of Cer6 on the gel-fluid phase transition of DEPE was very different from that of Cer16. Representative thermograms are shown in Fig. 9. Rather than shifting the transition toward higher temperatures, as did Cer16, Cer6

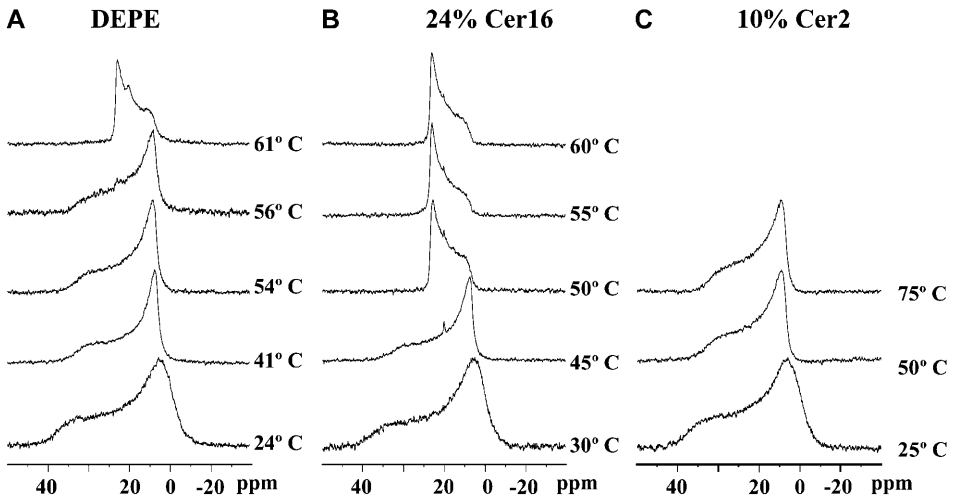

FIGURE 7 ^{31}P-NMR spectra of aqueous dispersions of pure DEPE and DEPE-ceramide mixtures. (*A*) Pure DEPE. (*B*) DEPE containing 24 mol % Cer16. (*C*) DEPE containing 10 mol % Cer2. Spectra were recorded at various temperatures, after 10 min sample equilibration, as indicated for each spectrum. Spectra were plotted with a line broadening of 40 Hz.

caused a decrease in the L_β-L_α transition temperature of DEPE. Note that, according to regular solution theory, Cer6 should increase the melting temperature of the mixture, since its melting point is above the T_c of pure DEPE. In fact, as little as 3 mol % Cer6 caused the appearance of a new endotherm at $T_m \approx 25°C$ (peak 5), indicating the presence of a novel phase that coexisted with the L_β phase of DEPE. Moreover, the main transition of DEPE became broadened toward the low-temperature side, the band decomposition showing as many as four component bands, corresponding to at least as many other compositionally distinct domains. Increasing proportions of Cer6 failed to induce further

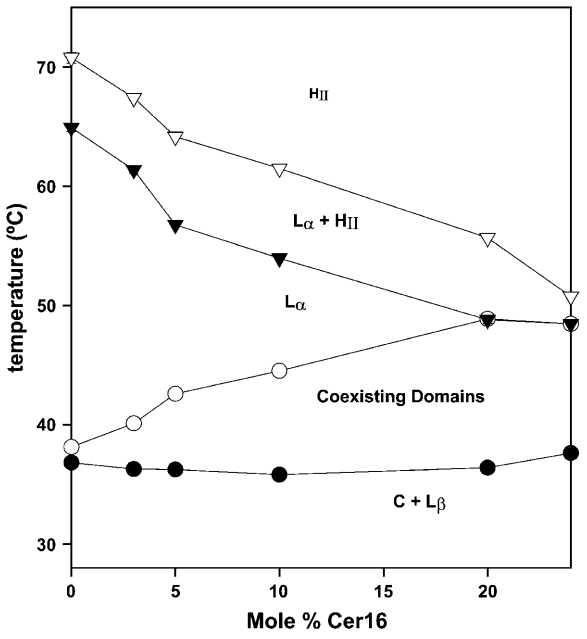

FIGURE 8 Temperature-composition diagram for the DEPE-Cer16 system in aqueous medium (excess water). Transition temperatures were derived from DSC thermograms (Figs. 1 and 3). Phase structures were obtained from x-ray diffraction (Figs. 5 and 6) and ^{31}P-NMR (Fig. 7) studies. *C*, ceramide-rich gel phase. L_β, DEPE, or DEPE-rich, gel phase. L_α, liquid-crystalline or fluid phase. H_{II}, inverted hexagonal phase. (●, ○) Respectively, onset and completion temperatures of the gel-fluid phase transition. (▼, ▽) Respectively, onset and completion temperatures of the lamellar-inverted hexagonal phase transition. Average values ± SD ($n = 3$). In most cases, the standard deviation is approximately the size of the symbols.

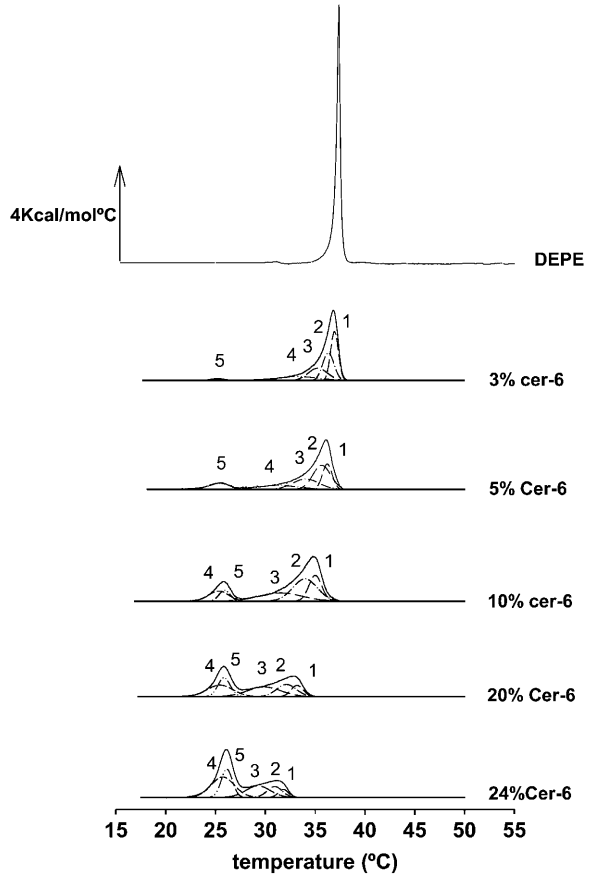

FIGURE 9 DSC thermograms corresponding to the gel-fluid transition of pure DEPE and DEPE-Cer6 mixtures in aqueous medium (third heating scans). DEPE concentration was the same (0.4 mM) in all samples. Dashed lines, transition components obtained with the GRAMS software.

significant shifts of component 5 to lower temperatures, showing that the phase responsible for component 5 did not mix with gel-phase DEPE. Instead, there was a gradual shift of peaks 1–4 toward lower temperatures and a concomitant decrease in the areas under the high T-peaks, with a corresponding increase in the low T-peaks. The presence of a novel phase associated to component 5 speaks in favor of an interaction between DEPE and Cer6 that did not exist between DEPE and Cer16. The gradual downshift of the onset temperature of the main transition indicates miscibility of the various ceramide-enriched domains among themselves, whereas the constant onset temperature of the low T-endotherm shows that the ceramide-rich domains do not mix with DEPE below 20°C. Thus Cer6, at variance with Cer16, can mix to some extent with DEPE in the 23–37°C temperature range.

The thermodynamic parameters of the gel-fluid transition of DEPE-Cer6 mixtures are summarized in Fig. 10. Because of the complex lineshape of the thermograms, data corresponding to the ''low T-peak'' and ''high T-peak'' are presented separately. The left-hand column (Fig. 10 *A*, *C*, and *E*) corresponds to the ''low T-peak'', i.e., component 5 and, for Cer6 concentrations ≥10 mol %, also component 4. Fig. 10 *A* also includes data for the total enthalpy change associated with the transition. As was the case for Cer16 (Fig. 2) inclusion of Cer6 in DEPE bilayers did not alter the overall transition ΔH (Fig. 10 *A*). However ΔH of the component peaks 4 and 5 increased gradually with Cer6 concentration, as was suggested by the decomposed thermograms in Fig. 9. Neither T_m nor $\Delta T_{1/2}$ of components 4 and 5 changed significantly with Cer6 concentration (Fig. 10 *C* and *E*).

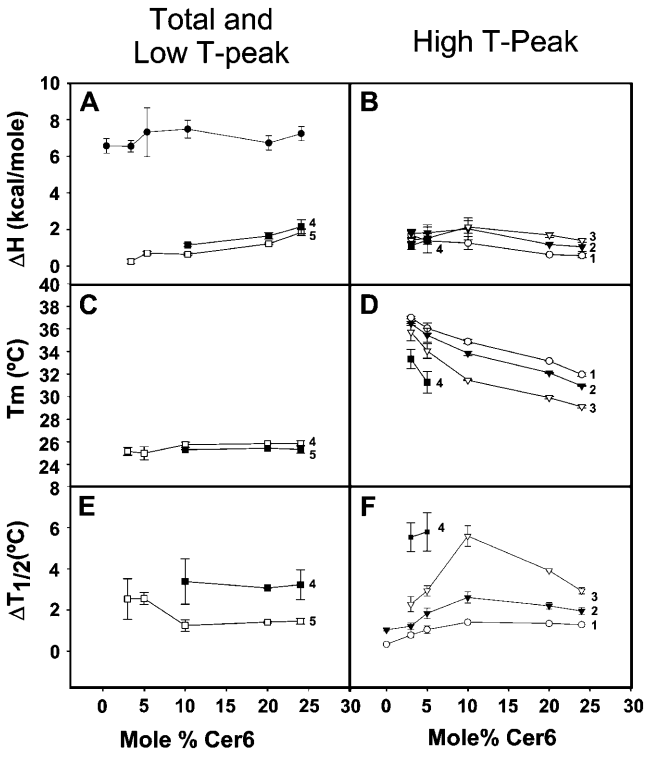

FIGURE 10 Thermodynamic parameters of the gel-fluid transition of pure DEPE and DEPE-Cer6 mixtures in aqueous medium. (*A* and *B*) Transition enthalpy change, ΔH. (*C* and *D*) Midpoint transition temperatures, T_m. (*E* and *F*) Transition widths at half-height, $\Delta T_{1/2}$. Average values ± SD ($n = 3$). (●) Total change in ΔH. The numbering 1–5 refers to the transition components shown in Fig. 7.

The components of the ''high T-peak'', i.e., components 1, 2, 3, and (at low Cer6 concentrations) 4, i.e., those arising from DEPE-rich domains, behaved differently. Both their ΔH and T_m tended to decrease, for the reasons explained above in connection with the thermograms in Fig. 9. The width of components 1 and 2 remained fairly constant, whereas that of component 3 first increased significantly, then decreased to the original value. This is probably an indication of the progressive enrichment in Cer6 of the various domains, those giving rise to peak component 3 constituting an intermediate situation between the DEPE-richer component 1 and the ceramide-richer component 5. It should be noted however, in the interpretation of these DEPE-Cer6 thermograms, that the presence of domains of various compositions in a two-component system may indicate that the system is not in thermal equilibrium. Even if this were the case, our results would undoubtedly indicate a degree of mixing of Cer6 with DEPE below 37°C.

Thermograms corresponding to the lamellar-to-inverted hexagonal transition of DEPE-Cer6 mixtures are shown in Fig. 11. The corresponding thermodynamic parameters are summarized in Fig. 12. Cer6 decreases the T_h transition temperature, i.e., it increases the propensity of DEPE to adopt the inverted hexagonal architecture, without significant changes in transition enthalpy or width. An interesting, yet unexplained, feature is that Cer6, at concentrations above 10 mol %, removes the high-T shoulder of the L_α-H_{II} transition of DEPE.

Thus Cer6 and Cer16 had opposite effects on the gel-fluid transition of DEPE, respectively lowering and rising the transition temperatures (Figs. 1 and 9). However, both ceramides lowered the L_α-H_{II} transition temperature (Figs. 3 and 11) although Cer16 was more potent in this respect. From the data in Figs. 4 and 12, ΔT_h was of ~−1°C/mol % Cer16, but of only −0.30°C/mol % Cer6. Figures from Veiga et al. (1999) were −1.3°C/mol % egg ceramide, and −10.8°C/mol % egg diacylglycerol (DEPE bilayers in all cases).

Fig. 5, *D* and *E*, shows the diffraction patterns corresponding to DEPE containing Cer6 at different temperatures. The presence of Cer6 promoted the appearance of the hexagonal H_{II} phase at temperatures lower than that of the pure phospholipid. At 61°C, pure DEPE is organized in a lamellar fluid phase (Fig. 5 *A*), whereas in the presence of 10 mol % Cer6, a mixture of lamellar fluid and hexagonal H_{II} phases are found (Fig. 5 *D*), and only hexagonal H_{II} phase is observed in the presence of 24 mol % Cer6 (Fig. 5 *E*). This is analogous to what it was found for Cer16 (Fig. 5, *B* and *C*), but Cer16 was clearly a better hexagonal H_{II} phase promoter

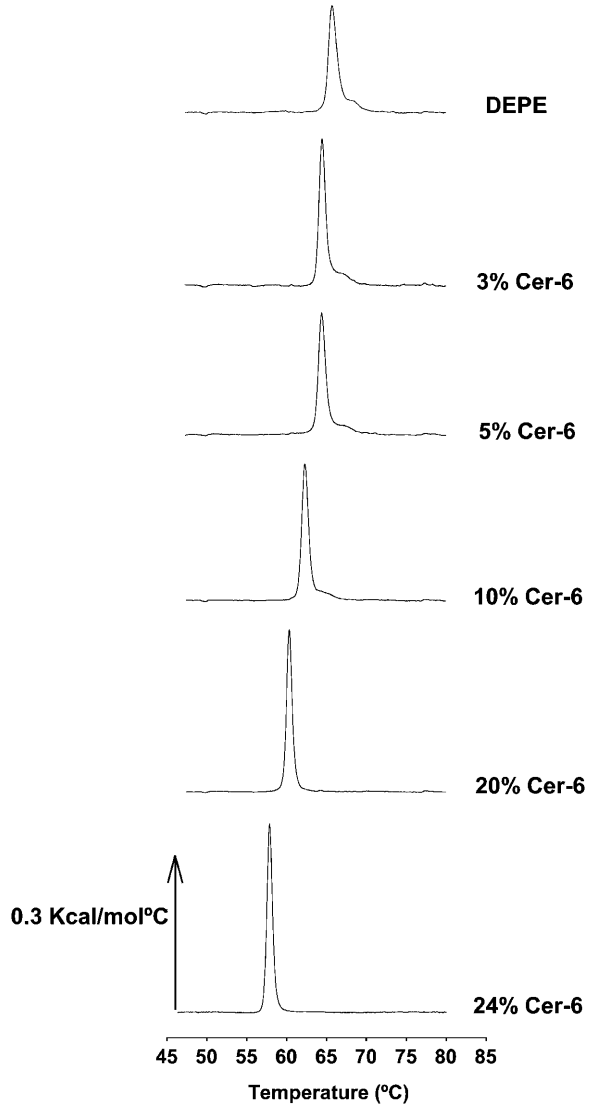

FIGURE 11 DSC thermograms corresponding to the lamellar-to-inverted hexagonal transition of pure DEPE and DEPE-Cer6 mixtures in aqueous medium (third heating scans). DEPE concentration was constant (7 mM) in all samples.

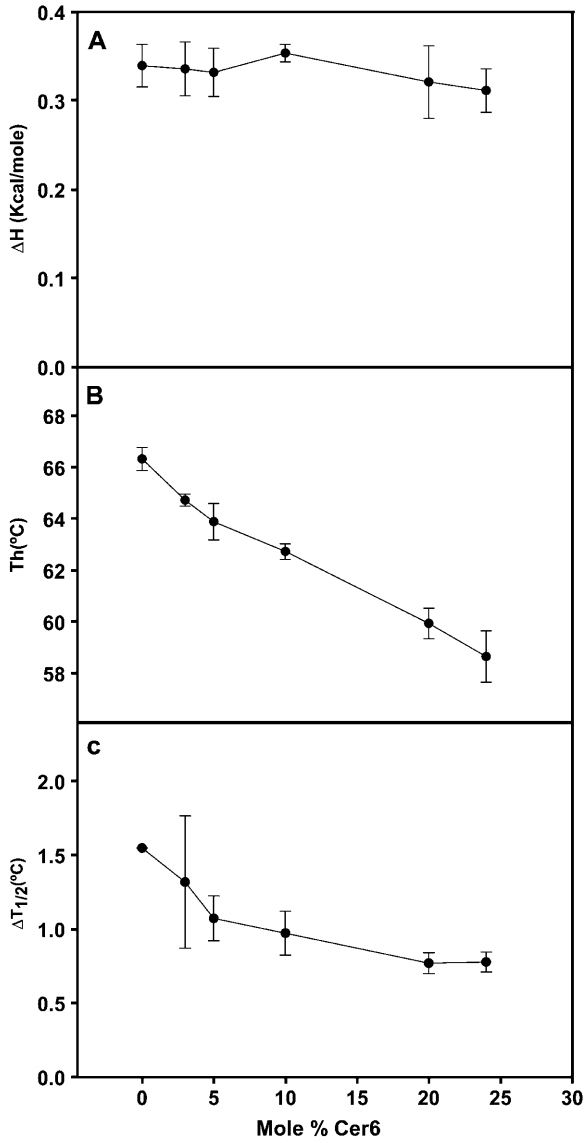

FIGURE 12 Thermodynamic parameters of the L_α-H_{II} transition of pure DEPE and DEPE-Cer6 mixtures in aqueous medium. (*A*) Transition enthalpy change, ΔH. (*B*) Midpoint hexagonal transition temperature, T_h. (*C*) Transition width at midheight, $\Delta T_{1/2}$. Average values ± SD ($n = 3$).

than Cer6 (Fig. 6). In the case of Cer6, we also observed a very weak reflection (more evident at temperatures at which the lipid is organized in the hexagonal H_{II} phase), which possibly might arise from a different lamellar phase similarly to the one described above (Fig. 6) for Cer16 although quantitatively less important.

The temperature-composition diagram (''phase diagram'') for DEPE-Cer6 mixtures in excess water is presented in Fig. 13. As soon as some Cer6 is present in the bilayer, a ceramide-enriched C gel phase is formed that coexists with the L_β phase of DEPE (the latter perhaps somewhat modified by the presence of small amounts of ceramide). Between ≈23°C and ≈37°C, multiple domains (components 1–5 in the thermograms in Fig. 9) coexist with increasing proportions of L_α phase. The latter becomes preponderant in the 38–56°C range, irrespective of ceramide concentration in the bilayers. Then, above 60–70°C, the inverted hexagonal H_{II} phase is formed, at a lower temperature the higher the proportion of Cer6. Still, the relatively low ability of Cer6 to decrease T_h ensures the presence of L_α phase at all Cer6 concentrations tested, unlike the situation for the DEPE-Cer16 mixture (Fig. 8).

Carrer et al. (2003) have published a calorimetric phase diagram for mixtures of dimyristoylphosphatidylcholine (DMPC) and Cer8, including only the gel-fluid transition. Although not exactly similar, their data resemble more the behavior of Cer16 (Fig. 8) than those of Cer6 (Fig. 13). The boundary between ''short'' and ''long'' ceramides is difficult to draw; some authors place it in the C6-C8 acyl

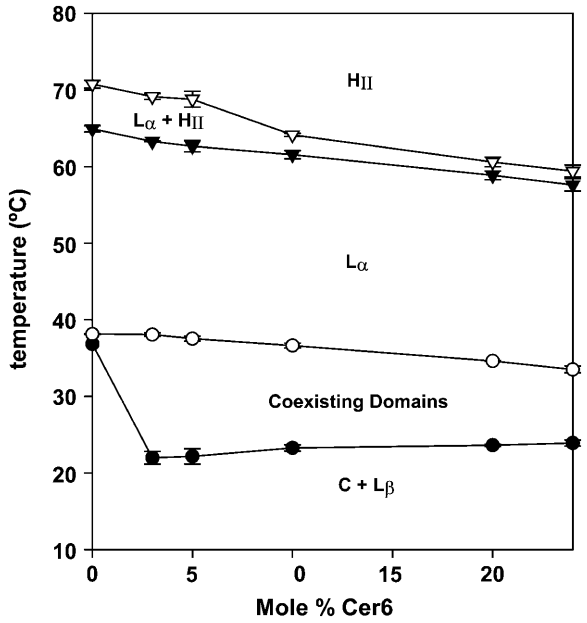

FIGURE 13 Temperature-composition diagram for the DEPE-Cer6 system in aqueous medium (excess water). (*C*) ceramide-rich gel phase. L_β, DEPE, or DEPE-rich, gel phase. L_α, liquid-crystalline or fluid phase. H_{II}, inverted hexagonal phase (●, ○) Respectively, onset and completion temperatures of the gel-fluid phase transition. (▼, ▽) Respectively, onset and completion temperatures of the lamellar-inverted hexagonal phase transition. Average values ± SD ($n = 3$). In most cases, the standard deviation is approximately the size of the symbols.

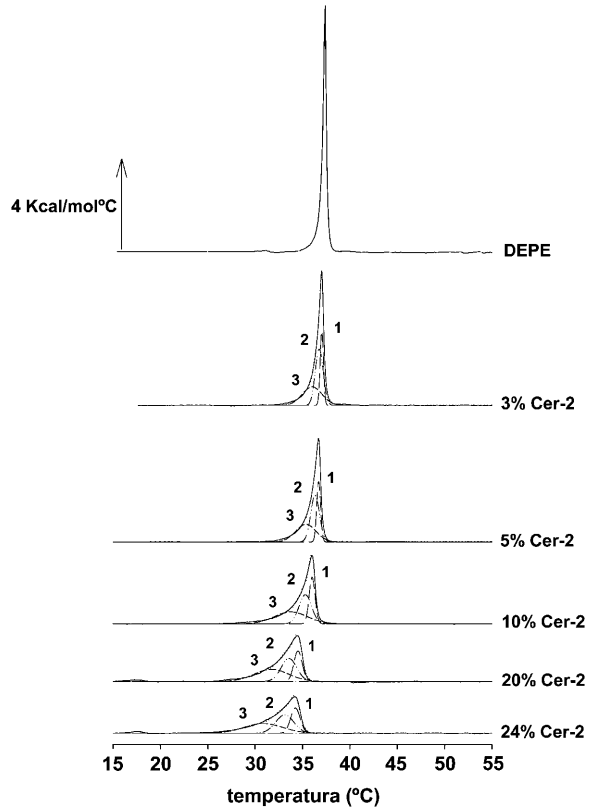

FIGURE 14 DSC thermograms corresponding to the gel-fluid transition of pure DEPE and DEPE-Cer2 mixtures in aqueous medium (third heating scans). DEPE concentration was the same (0.4 mM) in all samples. Dashed lines, transition components obtained with the GRAMS software.

chain region (Kolesnick et al., 2000) although it is evident that the relationship between ceramide and phospholipid acyl chain length will also influence the outcome of the interaction. In particular, the effect of a Cer8 on a dimyristoyl (C14) phosphatidylcholine bilayer may be more akin to that of a ''long-chain'' ceramide (e.g., Cer16) on a DEPE (C18) bilayer.

DEPE-Cer2 mixtures

Cer2 exerted characteristic effects on the gel-fluid and lamellar-hexagonal transitions of DEPE. Representative thermograms of the gel-fluid transition are depicted in Fig. 14. The main effect of Cer2 was to widen and downshift the transition. Both the onset and completion temperatures were shifted, suggesting that Cer2 mixed well in both the L_β and L_α phases of DEPE. The situation was reminiscent of that of the ''high T-peak'' in DEPE-Cer6 mixtures (In fact a faint endotherm was detected at 16–18°C, in mixtures containing ≥20 mol % Cer2, that could correspond to the ''low T-peak'' of DEPE-Cer6. This very small endotherm was not further analyzed). Cer2-induced widening of the gel-fluid DEPE transition was asymmetrical, with a progressively more pronounced shoulder being formed on the low T-side. Endotherm decomposition (Fig. 14, *dashed lines*) revealed the progressive conversion of a narrow, presumably DEPE-rich component 1 into a wide, ceramide-rich component 3. The order-disorder transition of Cer2 occurred at 54°C, i.e., above the gel-fluid transition of DEPE, and yet the ceramide lowered the transition temperature of the mixture, indicating nonideal mixing, due to some degree of interaction between both lipids. In fact Sot et al. (2005) have proposed that Cer2, and to a lower extent Cer6, have a detergent effect, converting part of the DEPE bilayer into DEPE-ceramide mixed micelles.

The above qualitative observations are expressed in a quantitative way in Fig. 15. Note that, at variance with its longer chain-analogs, Cer2 caused a gradual decrease in the overall transition enthalpy of the mixture (Fig. 15 *A*). T_m of the whole endotherm and of each of the component peaks decreased monotonically with Cer2 concentration (Fig. 15 *B*), whereas endotherm width was concomitantly increased (Fig. 15 *C*).

The L_α-H_{II} transition of DEPE in the presence of increasing amounts of Cer2 was also studied by DSC. Cer2 differed from both Cer16 and Cer6 in that it increased T_h, i.e., it stabilized the lamellar phase. This behavior can also be explained in the terms of the molecular shape theory of Israelachvili et al. (1980). Because of its very short N-acyl chain, the molecular cross section of the hydrophobic moiety of Cer2 is smaller than the cross section of the polar head group, i.e., Cer2 has a shape that favors ''positive curvature''

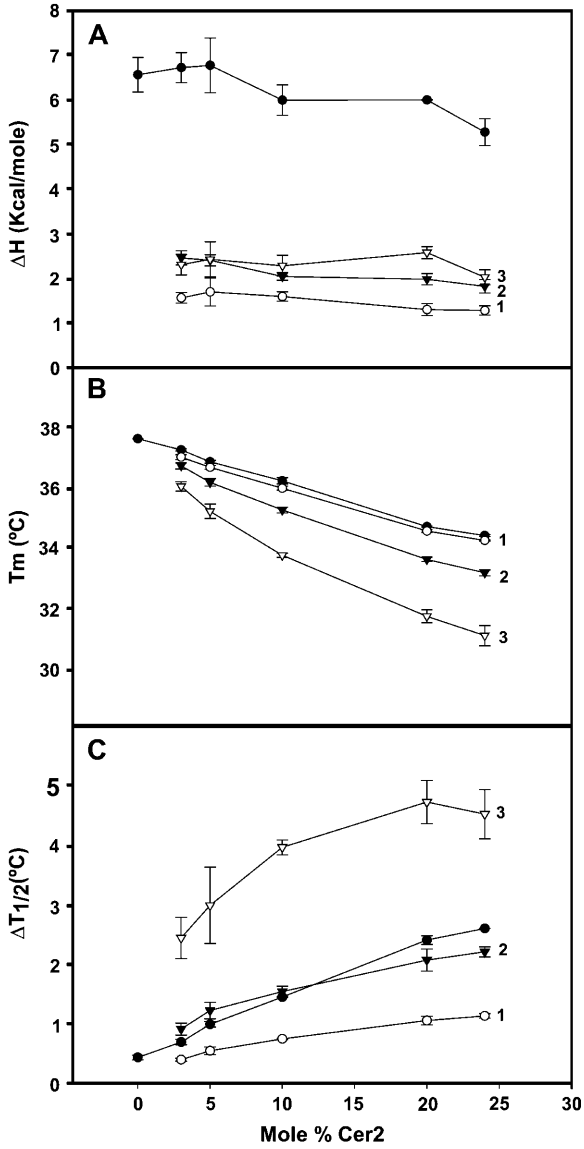

FIGURE 15 Thermodynamic parameters of the L_β-L_α transition of pure DEPE and DEPE-Cer2 mixtures in aqueous medium. (*A*) Transition enthalpy change, ΔH. (*B*) Midpoint transition temperature, T_m. (*C*) Transition width at midheight, $\Delta T_{1/2}$. (●) Data from the overall endotherm. (○) Component 1. (▼) Component 2. (▽) Component 3. Average values ± SD ($n = 3$).

of the monolayer (Helfrich, 1973), thus opposing the lamellar-to-inverted hexagonal transition. Note that Cer16 was described above as having the opposite geometrical properties. Moreover DEPE itself, like phosphatidyletanolamines in general, has a certain propensity to form inverted phases (Epand, 1985). Such a propensity is countered by the geometry of Cer2. Fig. 5 shows the diffraction patterns corresponding to pure DEPE and DEPE containing Cer2 at different temperatures. It is clearly seen that at 67°C, temperature at which the pure DEPE system is completely organized in the hexagonal H_{II} phase Fig. 5 *A*), the presence of Cer2 at different concentrations produced the appearance of reflections related as 1: 1/2: 1/3: 1/4 with a repeat distance of ~51 Å (Fig. 5, *F* and *G*) evidencing that the system is still organized in the lamellar fluid phase. The persistence of the lamellar phase in DEPE-Cer2 mixtures at temperatures as high as 75°C has also been demonstrated by ^{31}P-NMR studies (Fig. 7 *C*).

Various other lipids whose molecular geometry resembles that of Cer2 have been studied in mixtures with DEPE by Gómez-Fernández and co-workers. Platelet-activating factor (1-0-hexadecyl-*sn*-glycero-3-phosphocholine), its lyso-derivative (1-O-hexadecyl-*sn*-glycero-3-phosphocholine), 1-palmitoyl-*sn*-glycero-3-phosphocholine, and the antineoplastic ether lipid 1-O-octadecyl-2-O-methyl-glycero-3-phosphocholine, decrease the gel-fluid transition temperature of DEPE and diminish the associated ΔH. The same lipids, also in common with Cer2, act as typical molecules increasing T_h, i.e., stabilizing the lamellar versus the inverted hexagonal phase because of their propensity to favor positive monolayer curvature (Salgado et al., 1993; Sanchez-Pinera et al., 1999). In our laboratory, *N*-palmitoylcarnitine, also a lipid that favors positive curvature, was seen to decrease T_m and increase T_h of DEPE (Veiga et al., 1996). Thus the calorimetric behavior of Cer2 in mixtures with DEPE appears to follow a well-established pattern of molecules that favor positive curvature. Probably the same geometric considerations explain that all of the above molecules display a surfactant activity.

An additional important peculiarity of Cer2 is that, under the experimental conditions of this study, no equilibrium was reached by the DEPE-Cer2 mixtures above 60°C. In all other mixtures described in this study, thermograms were perfectly superimposable after the second heating scan. This was not the case with the DEPE-Cer2 thermograms. When these mixtures were repeatedly scanned, the transition was progressively shifted to higher temperatures, and its apparent associated enthalpy was concomitantly decreased (data not shown). Allowing the sample to equilibrate for several days at 4°C did not modify the behavior of this mixture. The temperature shift and the decrease in enthalpy with repeated scanning may be a consequence of gradual DEPE vesicle solubilization by Cer2, with the concomitant change in bilayer composition and curvature.

In summary, it is clear that the DEPE-Cer2 system above 60°C does not reach equilibrium under our conditions, thus any attempt at estimating the thermodynamic properties of the corresponding L_α-H_{II} transition would be meaningless. The nonequilibrium situation also makes impossible a proper temperature-composition diagram in the high *T*-region. Nevertheless, a partial diagram is presented in Fig. 16, with reliable data for the L_β-L_α region. Note that thermograms for the gel-fluid transition were perfectly reproducible from the second heating scan. In addition, a dotted line has been included in Fig. 16, based on the onset temperatures of the L_α-H_{II} transition in the second scans of these mixtures. The dotted line would represent the lowest boundary of the H_{II} phase.

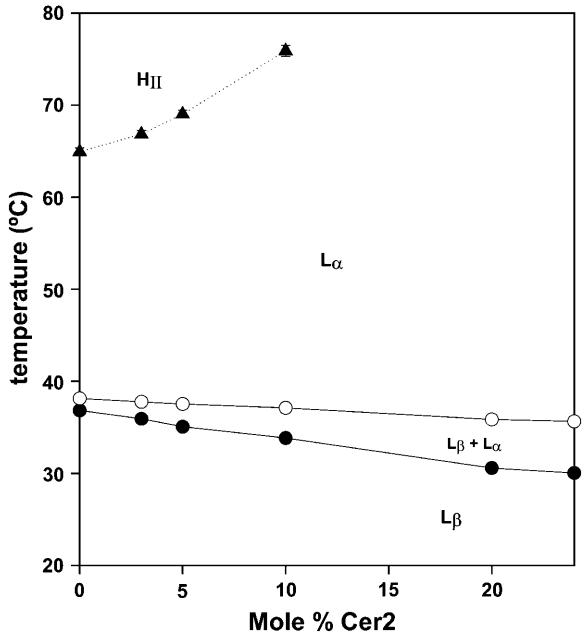

FIGURE 16 Temperature-composition diagram for the DEPE-Cer2 system in aqueous medium (excess water). L_β, gel phase. L_α, fluid phase. H_{II}, inverted hexagonal phase. (●, ○) Respectively, onset and completion temperatures of the gel-fluid phase transition, data from the third heating scan. (▼) Onset temperature of the L_α-H_{II} transition, data from the second heating scan. Average values ± SD ($n = 3$). In most cases, the standard deviation is smaller than the size of the symbol. The dotted line represents the lowest boundary of the H_{II} phase (see main text for details).

Mixtures with phospholipids other than DEPE

To confirm the validity of the above results, the effects of Cer16, Cer6, and Cer2 on the gel-fluid transition of phospholipids other than DEPE, namely DMPC and DPPC, were tested by DSC. In these experiments, 10 mol % ceramide were used in all cases. Both with DMPC and DPPC, the results were very similar to those described above for DEPE bilayers (thermograms not shown). Cer16 at 10 mol % caused a large increase in the width of the L_β-L_α transition of DMPC and DPPC, with the appearance of a high-temperature shoulder extending 5–8°C above the T_c of the pure phospholipid. Cer6, at 10 mol %, also widened the gel-fluid main transition, although to a lesser extent than Cer16. Importantly, Cer6 did not cause, neither in DMPC nor in DPPC, the split endotherm observed with DEPE (Fig. 9). Finally, 10 mol % Cer2 changed but slightly the main endotherm of the DMPC and DPPC gel-fluid transitions, a behavior similar to that observed in DEPE-Cer2 mixtures (Fig. 14). Neither DMPC nor DPPC can undergo a lamellar-hexagonal transition in the temperature range under study, thus the effect on phospholipids could not be evaluated. However in our previous study on ceramide effects on phospholipid membranes (Veiga et al., 1999), both egg and brain ceramides were tested on DEPE and on *N*-monomethyl dioleoylphosphtidylethanolamine (DOPE-Me) bilayers, with very similar effects, decrease in T_h and increase in ΔH. Our results with DEPE-Cer16 are also similar to those obtained by Hsueh et al. (2002) for POPC-Cer16. All these data support the idea that the ceramide effects described above in mixtures with DEPE occur as well in a variety of phospholipid matrices.

CONCLUDING REMARKS

The way in which the various ceramides perturb the gel-fluid (L_β-L_α) and lamellar-hexagonal (L_α-H_{II}) transitions of DEPE provides interesting insights on the behavior of ceramides in membranes, and specifically on ceramide-phospholipid interactions. The results in this study show essentially two modes of ceramide-phospholipid interaction, corresponding to the long- and short-chain ceramides. These are represented here by the *N*-hexadecanoyl (Cer16) and the *N*-acetyl (Cer2) sphingosines, respectively. Long-chain ceramides mix poorly with phospholipids in the gel phase, although they are solubilized in the fluid phase. In addition, they promote the lamellar-hexagonal transition. On the contrary, Cer2, as a representative of short-chain ceramides, mixed well in the gel phase phospholipid and stabilized the fluid phase, both by lowering the gel-fluid and by increasing the lamellar-hexagonal transition temperatures. *N*-hexanoyl sphingosine (Cer6) displayed intermediate properties between Cer16 and Cer2: it lowered the gel-fluid and the lamellar-hexagonal transition temperatures of the phospholipid. The easiest way to rationalize the above results is to take into account the molecular geometry of the ceramides (Helfrich, 1973; Israelachvili et al., 1980). Because of the sphingosine and fatty acid chain-length mismatch, the cross-section of the hydrophobic moiety of Cer2 is smaller than the cross-section of its polar headgroup, thus Cer2 has a shape that favors the positive curvature of monolayers and the formation of micelles and opposes formation of inverted phases such as the H_{II}-inverted hexagonal. The opposite is true of Cer16: its shape favors negative curvature, and formation of inverted phases, e.g., H_{II}. It is remarkable that short- and long-chain ceramides often display equivalent physiological effects when added to cell systems, the reason being that many ceramide effects appear to reside mainly in the characteristic polar headgroup, perhaps through specific binding to target enzymes. However, there are cases in which both kinds of ceramides do have different cell effects (Guidoni et al., 1999; Di Paola et al., 2000). This could be an indication that the specific ceramide physiological effect under study is mediated by changes in the membrane physical properties. In the latter cases, it would be erroneous to consider the short-chain ceramides as ''analogs'' of their long-chain counterparts.

This work was supported in part by grants from Ministerio de Educación y Ciencia (BCM 2002-00784) and Universidad del País Vasco (UPV 00042.310/13552). J. Sot was a predoctoral student supported by the Basque government.

REFERENCES

Basañez, G., J. L. Nieva, E. Rivas, A. Alonso, and F. M. Goni. 1996. Diacylglycerol and the promotion of lamellar-hexagonal and lamellar-isotropic phase transitions in lipids: implications for membrane fusion. *Biophys. J.* 70:2299–2306.

Carrer, D. C., S. Hartel, H. L. Monaco, and B. Maggio. 2003. Ceramide modulates the lipid membrane organization at molecular and supramolecular levels. *Chem. Phys. Lipids.* 122:147–152.

Carrer, D. C., and B. Maggio. 1999. Phase behavior and molecular interactions in mixtures of ceramide with dipalmitoylphosphatidylcholine. *J. Lipid Res.* 40:1978–1989.

Castresana, J., J. L. Nieva, E. Rivas, and A. Alonso. 1992. Partial dehydration of phosphatidylethanolamine phosphate groups during hexagonal phase formation, as seen by i.r. spectroscopy. *Biochem. J.* 282:467–470.

Contreras, F. X., G. Basañez, A. Alonso, A. Herrmann, and F. M. Goñi. 2005. Ceramides promote transbilayer (flip-flop) lipid motion in membranes. *Biophys. J.* 88:348–359.

Contreras, F. X., A. V. Villar, A. Alonso, R. N. Kolesnick, and F. M. Goni. 2003. Sphingomyelinase activity causes transbilayer lipid translocation in model and cell membranes. *J. Biol. Chem.* 278:37169–37174.

Cremesti, A. E., F. M. Goni, and R. Kolesnick. 2002. Role of sphingomyelinase and ceramide in modulating rafts: do biophysical properties determine biologic outcome? *FEBS Lett.* 531:47–53.

Di Paola, M., T. Cocco, and M. Lorusso. 2000. Ceramide interaction with the respiratory chain of heart mitochondria. *Biochemistry.* 39:6660–6668.

Epand, R. M. 1985. Diacylglycerols, lysolecithin, or hydrocarbons markedly alter the bilayer to hexagonal phase transition temperature of phosphatidylethanolamines. *Biochemistry.* 24:7092–7095.

Epand, R. M., and C. T. Lemay. 1993. Lipid concentration affects the kinetic stability of dielaidoylphosphatdylethanolamine bilayers. *Chem. Phys. Lipids.* 66:181–187.

Guidoni, R., G. Sala, and A. Giuliani. 1999. Use of sphingolipid analogs: benefits and risks. *Biochim. Biophys. Acta.* 1439:17–39.

Han, C., R. Sanftleben, and T. S. Wiedmann. 1995. Phase properties of mixtures of ceramides. *Lipids.* 30:121–128.

Helfrich, W. 1973. Elastic properties of lipid bilayers: theory and possible experiments. *Z. Naturforsch. [C].* 28:693–703.

Holopainen, J. M., J. Y. Lehtonen, and P. K. Kinnunen. 1997. Lipid microdomains in dimyristoylphosphatidylcholine-ceramide liposomes. *Chem. Phys. Lipids.* 88:1–13.

Holopainen, J. M., M. Subramanian, and P. K. Kinnunen. 1998. Sphingomyelinase induces lipid microdomain formation in a fluid phosphatidylcholine/sphingomyelin membrane. *Biochemistry.* 37:17562–17570.

Hsueh, Y. W., R. Giles, N. Kitson, and J. Thewalt. 2002. The effect of ceramide on phosphatidylcholine membranes: a deuterium NMR study. *Biophys. J.* 82:3089–3095.

Huang, H. W., E. M. Goldberg, and R. Zidovetzki. 1996. Ceramide induces structural defects into phosphatidylcholine bilayers and activates phospholipase A2. *Biochem. Biophys. Res. Commun.* 220:834–838.

Huang, H. W., E. M. Goldberg, and R. Zidovetzki. 1998. Ceramides perturb the structure of phosphatidylcholine bilayers and modulate the activity of phospholipase A2. *Eur. Biophys. J.* 27:361–366.

Israelachvili, J. N., S. Marcelja, and R. G. Horn. 1980. Physical principles of membrane organization. *Q. Rev. Biophys.* 13:121–200.

Killian, J. A., and B. de Kruijff. 1985. Thermodynamic, motional and structural aspects of gramicidin-induced hexagonal H_{II} phase formation in phosphatidylethanolamine. *Biochemistry.* 24:7881–7890.

Kolesnick, R. N., F. M. Goni, and A. Alonso. 2000. Compartmentalization of ceramide signalling: physical foundations and biological effects. *J. Cell. Physiol.* 184:285–300.

Luzzati, V. 1968. X-ray diffraction studies of lipid-water systems. *In* Biological Membranes. D. Chapman, editor. Academic Press, New York. 71–123.

Massey, J. B. 2001. Interaction of ceramides with phosphatidylcholine, sphingomyelin and sphingomyelin/cholesterol bilayers. *Biochim. Biophys. Acta.* 1510:167–184.

Montes, L. R., M. B. Ruiz-Arguello, F. M. Goni, and A. Alonso. 2002. Membrane restructuring via ceramide results in enhanced solute efflux. *J. Biol. Chem.* 277:11788–11794.

Moore, D. J., and M. E. Rerek. 1997. Lipid domains and orthorhombic phases in model stratum corneum: evidence from Fourier transform infrared spectroscopy studies. *Biochem. Biophys. Res. Commun.* 231: 797–801.

Ortiz, A., and F. J. Aranda. 1999. The influence of vitamin K1 on the structure and phase behaviour of model membrane systems. *Biochim. Biophys. Acta.* 1418:206–220.

Pascher, I. 1976. Molecular arrangements in sphingolipids. Conformation and hydrogen bonding of ceramide and their implication on membrane stability and permeability. *Biochim. Biophys. Acta.* 455:433–451.

Ruiz-Argüello, M. B., G. Basanez, F. M. Goni, and A. Alonso. 1996. Different effects of enzyme-generated ceramides and diacylglycerols in phospholipid membrane fusion and leakage. *J. Biol. Chem.* 271:26616–26621.

Ruiz-Argüello, M. B., F. M. Goni, and A. Alonso. 1998. Vesicle membrane fusion induced by the concerted activities of sphingomyelinase and phospholipase C. *J. Biol. Chem.* 273:22977–22982.

Salgado, J., J. Villalain, and J. C. Gomez-Fernandez. 1993. Effects of platelet-activating factor and related lipids on dielaidoylphosphatidylethanolamine by DSC, FTIR and NMR. *Biochim. Biophys. Acta.* 1145: 284–292.

Sanchez-Pinera, P., F. J. Aranda, V. Micol, A. de Godos, and J. C. Gomez-Fernandez. 1999. Modulation of polymorphic properties of dielaidoylphosphatidylethanolamine by the antineoplastic ether lipid 1-O-octadecyl-2-O-methyl-glycero-3-phosphocholine. *Biochim. Biophys. Acta.* 1417:202–210.

Shah, J., J. M. Atienza, R. I. Duclos Jr., A. V. Rawlings, Z. Dong, and G. G. Shipley. 1995. Structural and thermotropic properties of synthetic C16:0 (palmitoyl) ceramide: effect of hydration. *J. Lipid Res.* 36:1936–1944.

Siegel, D. P., and R. M. Epand. 1997. The mechanism of lamellar-to-inverted hexagonal phase transitions in phosphatidylethanolamine: implications for membrane fusion mechanisms. *Biophys. J.* 73:3089–3111.

Siskind, L. J., and M. Colombini. 2000. The lipids C2- and C16-ceramide form large stable channels. Implications for apoptosis. *J. Biol. Chem.* 275:38640–38644.

Siskind, L. J., R. N. Kolesnick, and M. Colombini. 2002. Ceramide channels increase the permeability of the mitochondrial outer membrane to small proteins. *J. Biol. Chem.* 277:26796–26803.

Sot, J., F. M. Goni, and A. Alonso. 2005. Molecular associations and surface-active properties of short- and long-*N*-acyl chain ceramides. *Biochim. Biophys. Acta.* In press.

Stoffel, W. 1971. Sphingolipids. *Annu. Rev. Biochem.* 40:57–82.

Van Blitterswijk, W. J., A. van der Luit, R. J. Veldman, M. Verheij, and J. Borst. 2003. Ceramide: second messenger or modulator of membrane structure and dynamics? *Biochem. J.* 369:199–211.

Veiga, M. P., J. L. Arrondo, F. M. Goni, and A. Alonso. 1999. Ceramides in phospholipid membranes: effects on bilayer stability and transition to nonlamellar phases. *Biophys. J.* 76:342–350.

Veiga, M. P., M. A. Requero, F. M. Goni, and A. Alonso. 1996. Effect of long-chain acyl-CoAs and acylcarnitines on gel-fluid and lamellar-hexagonal phospholipid phase transitions. *Mol. Membr. Biol.* 13:165–172.

Wiegandt, H. 1970. Gangliosides of extraneuronal tissue. *Chem. Phys. Lipids.* 5:198–204.